PRINT ISSN 1119-8362
Electronic ISSN 2659-1499

Full-text Available Online at
https://www.ajol.info/index.php/jasem
https://www.bioline.org.br/ja

J. Appl. Sci. Environ. Manage.
Vol. 28 (3) 665-674 March 2024

Soil Adjusted Vegetation Index, Normalize Difference Buildup Index, and Land Surface Temperature between 1987 and 2023 in Abuja Municipal Area Council, Nigeria

***[1]OKODUWA, KA; [1]AMAECHI, CF; [1, 2]ENUNEKU, AA**

[1]Department of Environmental Management and Toxicology, Faculty of Life Sciences, University of Benin, PMB 1154, Benin City, Nigeria.
[2] Laboratory for Ecotoxicology and Environmental Forensics, University of Benin, PMB 1154, Benin City, Nigeria.

**Corresponding Author Email: akus.okoduwa@lifesci.uniben.edu*
**ORCID ID: https://orcid.org/0009-0001-6469-4668*

Co-Authors Email: chika.amaechi@uniben.edu; alex.enuneku@uniben.edu

ABSTRACT: Abuja Municipal Area Council (AMAC) is experiencing rapid urban expansion, which is expected to impact land surface temperatures (LST). This paper evaluates the trends in soil adjusted vegetation index (SAVI), normalize difference buildup index (NDBI), and land surface temperature (LST) between 1987 and 2023 in AMAC using Landsat 4 Thematic Mapper and Landsat 8 Operational Land Imager/Thermal Infrared Sensor imagery, respectively. Results show that in 1987, SAVI ranged from -0.126 to 0.477, NDBI from -0.186 to 0.678, and LST from 27.18 to 46.4 ºC. In 2023, SAVI ranged from -0.253 to 0.71, NDBI from -0.308 to 0.619, and LST from 23.89 to 46.57 ºC. Analysis showed an increase in vegetation in 2023 compared to 1987. Built-up and bareland areas became more concentrated in the northeast in 2023 compared to 1987, and temperature reductions were observed in areas with increased vegetation, notably in the south and southwest. Correlation analysis indicated a strong negative relationship (-0.772) between SAVI and LST in 1987, weakening in 2023 (-0.389). NDBI and LST remained moderately positively correlated (0.645 in 1987, 0.621 in 2023). Significant differences ($P<0.01$) were observed between 1987 and 2023 SAVI, NDBI, and LST values. These findings have important implications for environmental monitoring, and urban planning in rapidly urbanizing areas such as AMAC.

DOI: https://dx.doi.org/10.4314/jasem.v28i3.6

Cite this Article as: OKODUWA, K. A; AMAECHI, CF; ENUNEKU, A. A (2024) Soil Adjusted Vegetation Index, Normalize Difference Buildup Index, and Land Surface Temperature between 1987 and 2023 in Abuja Municipal Area Council, Nigeria. *J. Appl. Sci. Environ. Manage.* 28 (3) 665-674

Dates: Received: 18 January 2024; Revised: 24 February 2024; Accepted: 12 March 2024; Published: 29 March 2024

Keywords: Remote sensing; soil adjusted vegetation index; normalize difference buildup index; land surface temperature

Cities have grown from tiny, isolated population centers to huge urban centers during the past century (Fabolude and Aighewi, 2022; Amaechi *et al*., 2023). These growths involve the replacement of naturally occurring surfaces with highly reflective concrete masses, parking lots, asphalt roads, and other surfaces that have an impact on the urban temperature (Usman and Lay, 2013). According to Kolokotroni *et al.* (2006), urban temperature is growing globally, and reduced greenery in cities may be one of the contributing factors (Qiu *et al*., 2013; Kumar and Shekhar, 2015; Arifin *et al*., 2022). Researchers can gain valuable insights into the complex interactions between urbanization and temperature dynamics by utilizing remote sensing technology (Mohan and Kandya, 2015; Fu *et al.*, 2016; Saleem *et al*., 2020). The advantages of using remote-sensing data are the availability of high resolution, reliable and repetitive coverage, and proficiency of measurements of earth surface conditions (Ifatimehin and Magaji, 2009).

**Corresponding Author Email: akus.okoduwa@lifesci.uniben.edu*
**ORCID ID: https://orcid.org/0009-0001-6469-4668*

Remote sensing is a very reliable method for obtaining a better understanding of the earth's environment (Ahmadi and Nusrath, 2012; Li *et al*., 2020). It is the science and art of acquiring information and extracting features about any region without coming into physical contact with the region (Karaburun and Bhandari, 2010). For example, SAVI can be used to estimate vegetation cover in any region (Vani and Mandla, 2017; Andhale *et al*., 2020; Rhyma *et al*., 2020). NDBI can be used to estimate built-up environments (Hari, 2018; Guha *et al*., 2018; Yasin *et al*., 2020), and thermal infrared (TIR) sensors can provide quantitative information regarding LST in various land cover classes (Dar *et al*., 2019; Malik *et al*., 2019; Ru *et al*., 2021). In several parts of the world, some authors with remotely sensed data have investigated the link between land cover classes and LST. For instance, Xian and Crane (2006) used Landsat Thematic Mapper (TM) and Enhanced Thematic Mapper Plus (ETM+) data to analyze the influence of urbanization on surface temperature in Tampa Bay, Florida. In addition, Faqe Ibrahim (2017) carried out a similar study in Dohuk City, Iraq, and reported high temperatures for bareland and built-up areas in 1990, 2000, and 2016 with values of 47 ºC, 50 ºC, and 56 ºC, respectively, while also reporting that the years 1990, 2000, and 2016 presented lower temperatures in relation to water bodies and forests with values of 25 ºC, 26 ºC, and 29 ºC, respectively.

In Nigeria, several researchers have carried out similar studies. Notable among them is Ifatimehin *et al*. (2009) who assessed the impact of land cover classes on the LST in Lokoja, Nigeria. Their findings showed that as the built-up area and bareland grew in extent, so did the surface temperature. This result clearly shows that built-up has a higher LST than other land cover classes. Similarly, Babalola and Akinsanola (2016) analyzed the spatial distribution of changes in LST and land cover using Landsat images in Lagos. The findings demonstrated that vegetative cover declined rapidly over 30 years, from 70.043% to 10.127%; this change contributed to changes in microclimate as urban and bare areas correlated positively with high LST. Adewale and Martins (2019) examine the relationship between urban growth and LST in AMAC using remote sensing techniques. They reported the mean LST of buildup areas as 27 ºC, 33 ºC, and 36 ºC in 1986, 2001, and 2016, respectively, with the highest temperature value at the city centre due to limited vegetative cover. As AMAC continues to develop, current research is needed to assess temperature variation and the spatial distribution of vegetation cover and built-up/bareland area using indices like SAVI and NDBI in order to plan for sustainable urban development as significant studies has not been carried out on AMAC. In view of the foregoing, the objective of this study was to evaluate the trends in soil adjusted vegetation index (SAVI), normalize difference buildup index (NDBI), and land surface temperature (LST) between 1987 and 2023 in Abuja Municipal Area Council, FCT Nigeria.

MATERIALS AND METHODS

Study Area: Abuja is Nigeria's federal capital territory; the research area AMAC (Figure 1) is one of Abuja's area councils.

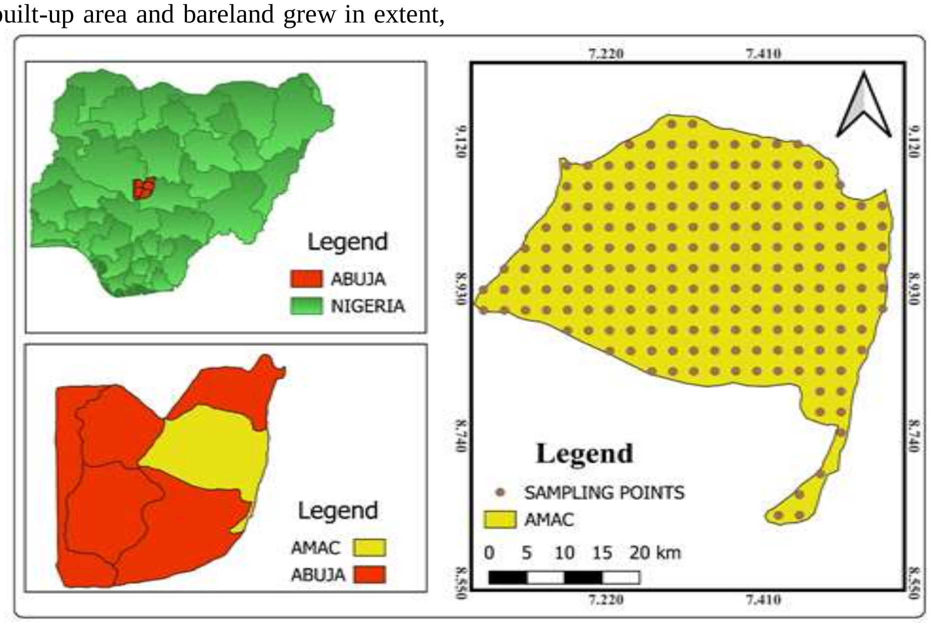

Fig 1. Map of Abuja Municipal Area Council showing sampling points used for statistical analysis (Source: Researchers work)

AMAC is the largest and most urbanized area in Abuja's six area councils (Touristlink, 2013). AMAC is situated between latitudes 8º36' N and 9º21' N of the Equator, and longitudes 7º07' E and 7º33' E of the

Greenwich Meridian (Adewale and Martins, 2019). It accounts for approximately 1,500 square kilometers (38.8%) of the entire land area of the Federal Capital Territory (FCT) (Balogun, 2001). The area is regarded as the most favorable and conducive for human habitation and settlement growth within the FCT (Mabogunje, 1976). The area has warm, humid rainy season and the chilly dry season. The rainy season lasts from April to October, with temperatures ranging from 28°C to 30°C during the day and 22°C to 23°C at night. In the dry season, it can get as high as 38°C during the day and as low as 12°C at night (Adeyeri *et al*., 2015). The total annual rainfall ranges from 1100 mm to 1600 mm, with relative humidity at 30% in the dry season and 70% in the wet season (Malik, 2004). AMAC has the largest population in Abuja, with 778,567 people, according to the 2006 National Population and Housing Census (NPC, 2006). The 2017 projected population of AMAC is roughly 1,967,500 (National Bureau of Statistics, 2017). The increasing rate of settlement expansion in AMAC is very likely to affect surface temperature due to deforestation, road construction, and industrial pollution (Adewale and Martins, 2019).

Image Acquisition: 30m-resolution Landsat images for 1987 and 2023 were obtained from the United States Geological Survey Earth Explorer site (https://earthexplorer.usgs.gov). To obtain images without cloud cover, a thorough study was performed, and it was discovered that LANDSAT 4TM (Thematic Mapper) from 1987-12-21 appears to have cloud cover and a land cloud cover of zero (0). Similarly, Landsat 8 (OLI/TIRS) (Operational Land Imager/Thermal Infrared Sensor) from 2023-12-16 appears to have cloud cover and a land cloud cover of 0.05, making it appropriate for this study.

After setting the appropriate search criteria, the images with path (189) and row (054) were downloaded in GeoTIFF format (.tif). The Landsat images downloaded are atmospherically corrected level-2 products, which have UTM (Universal Transverse Mercator) projection and WGS84 (World Geodetic System) datum. The acquired satellite images were processed in the geospatial tool ArcGIS 10.7. Then the region of interest (AMAC) was extracted from the entire scene using the Extract by Mask tool.

Observing 1987 and 2023 false color composite image: The first step to image classification should be a proper monitoring of the area with different band combinations to get familiar with the different land cover classes that exist in the area. After creating a band composite, a false-color composite was used to observe different land cover. From Fig. 2, the red cover represents vegetation, darker shades of blue represent water bodies, bright white or light grey represents buildup and varying shades of dark brown or black represent bareland. It was noticed that although the built-up area increased around the northeast region, vegetation cover also increased in the southwest region between 1987 and 2023 at the expense of bareland.

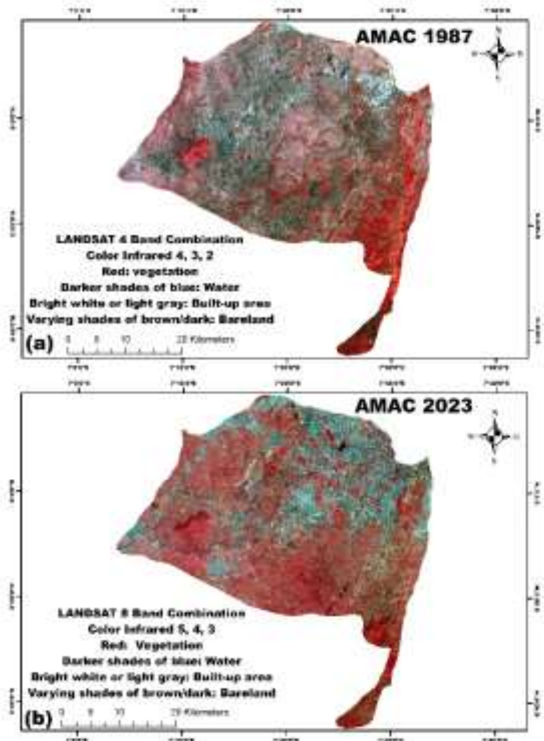

Fig 2: a (1987) and b (2023) false-color composite image (Source: Researchers work)

SAVI Calculation from Landsat 4 and Landsat 8 (Huete, 1988)

$$\text{SAVI} = \left(\left(\frac{\text{NIR} - \text{RED}}{\text{NIR} + \text{RED} + \text{L}}\right)\right) * (1 + \text{L}) \quad 1$$

For Landsat 4 SAVI

$$= \left(\left(\frac{\text{Band 4} - \text{Band 3}}{\text{Band 4} + \text{Band 3} + 0.5}\right)\right) * (1.5) \quad 2$$

For Landsat 8 SAVI

$$= \left(\left(\frac{\text{Band 5} - \text{Band 4}}{\text{Band 5} + \text{Band 4} + 0.5}\right)\right) * (1.5) \quad 3$$

L = soil brightness correction factor (0.5)

NDBI *Calculation from Landsat 4 and Landsat 8* (Zha *et al*., 2003)

$$\mathrm{NDBI} = \frac{\mathrm{SWIR} - \mathrm{NIR}}{\mathrm{SWIR} + \mathrm{NIR}} \quad 4$$

$$\text{For Landsat 4 NDBI} = \frac{\text{Band 5} - \text{Band 4}}{\text{Band 5} + \text{Band 4}} \quad 5$$

$$\text{For Landsat 8 NDBI} = \frac{\text{Band 6} - \text{Band 5}}{\text{Band 6} + \text{Band 5}} \quad 6$$

LST Retrieval from Landsat 4

Step 1: Conversion of Landsat Image Digital Number (DN) to radiance (Zareie *et al*., 2016)

$$L_\lambda = \left(\frac{\mathrm{LMAX}_\lambda - \mathrm{LMIN}_\lambda}{\mathrm{Qcal\ max} - \mathrm{Q\ cal\ min}}\right) \times (\mathrm{Qcal} - \mathrm{Qcal\ min}) + \mathrm{LMIN}_\lambda \quad 7$$

L_λ= Top of Atmospheric spectral radiance [watts/(m^2 srad µm)]; LMAX_λ = ADIANCE_MAXIMUM_BAND_6 = 15.303; LMIN_λ = RADIANCE_MINIMUM_BAND_6 = 1.238; Qcal = Landsat Image Digital Number (DN) =Band 6; Qcalmin = QUANTIZE_CAL_MIN_BAND_6 = 1; Qcalmax = QUANTIZE_CAL_MAX_BAND_6 = 255

Step 2: Conversion of radiance to brightness temperature (Landsat 7 Science Data Users Handbook, 2010; Guha *et al*., 2020)

$$\mathrm{BT} = \frac{K_2}{\left(\ln\left(\frac{K_1}{L_\lambda} + 1\right)\right.} \quad 8$$

BT = brightness temperature in Kelvin; L_λ = Top of Atmospheric spectral radiance; K_1 = K_1 Constant Band (671.62) (Watts/(m^2 * sr * µm)); K_2= K_2 Constant Band (1284.30) (Kelvin)

Step 3: Convert kelvin to Degree Celsius (°C)

$$o_C = \text{BT in Kelvin} - 273.15 \quad 9$$

LST Retrieval from Landsat 8

Thermal Infrared Digital Numbers can be transformed to TOA spectral radiance by applying the radiance rescaling factor (Anandababu *et al*., 2018):

Step 1: Calculating Top of Atmospheric Radiance (TOA)

$$L_\lambda = \mathrm{ML} * \mathrm{Qcal} + \mathrm{AL} \quad 10$$

L_λ = TOA spectral radiance [watts/(m^2 srad µm)]; ML = Radiance Multiplication Band 10 = 3.3420E-04; AL = Radiance Add Band 10 = 0.10000; Qcal = Quantized and calibrated standard product pixel values (DN) (BAND 10)

Step 2: Brightness Temperature: The thermal constant values is used to convert spectral radiance data to brightness temperature (Avdan and Jovanovska, 2016)

$$\mathrm{BT} = \frac{K_2}{\left(\ln\left(\frac{K_1}{L_\lambda} + 1\right) - 273.15\right.} \quad 11$$

BT = TOA Brightness Temperature (°C); L_λ = TOA spectral radiance; K_1 = K_1 Constant Band (774.8853); K_2= K_2 Constant Band (1321.0789)

The Landsat metadata file is where the values for LMIN, LMAX, QCALMIN, QCALMAX, K_1, and K_2, ML, and AL come from.

Step 3: Calculating NDVI: The Normalized Difference Vegetation Index (NDVI) is calculated with Near Infrared (Band 5) and Red (Band 4) bands. The NDVI is important because it assesses the amount of vegetation, which is a key factor in determining total vegetation health (Huang *et al* 2021). The estimation of NDVI is critical because it serves as the foundation for measuring the proportion of vegetation (PV). The correlation between NDVI, PV, and emissivity (ε) highlights the significance of computing these metrics together (Twumasi *et al*., 2021).

$$\mathrm{NDVI} = \frac{\mathrm{Nir\ (Band\ 5)} - \mathrm{Red\ (Band\ 4)}}{\mathrm{Nir\ (Band\ 5)} + \mathrm{Red\ (Band\ 4)}} \quad 12$$

Step 4: Calculating Vegetation Proportion **(**Wang *et al*., 2015)

$$\mathrm{Pv} = \left(\frac{\mathrm{NDVI} -}{\mathrm{NDVI}_{max} +}\frac{\mathrm{NDVI}_{min}}{\mathrm{NDVI}_{min}}\right)^2 \quad 13$$

Where PV= Proportion of vegetation; NDVI = DN values from the image; NDVI min = Minimum DN values from the image; NDVI max = Maximum DN values from NDVI image

Step 5: Calculating Land surface emissivity: It is necessary to calculate land surface emissivity (LSE) in order to estimate land surface temperature (Avdan and Jovanovska, 2016).

$$\varepsilon = 0.004 * \mathrm{PV} + 0.986 \quad 14$$

Where ε = Land surface emissivity; PV= Proportion of vegetation

Step 6: Calculating Land Surface Temperature

The Land Surface Temperature (LST) calculated using BT in ^{O}C, Wavelength of Emitted Radiance (w), and Land Surface Emissivity (ε) (Le Joseph, 2020).

$$LST = (BT / 1) + W \times (BT / 14380) \times \ln(\varepsilon) \quad 15$$

Extracting SAVI, NDBI, and LST values from raster image: In order to perform correlation analysis and check the level of significant difference, multiple values were extracted from the SAVI, NDBI, and LST raster images using the Fishnet tool in ArcMap. To remove the null values (0 and -999), the Fishnet points generated were clipped with an AMAC shapefile. The values generated were imported to Excel to make tables and to SPSS (Statistical Package for the Social Sciences) for Pearson correlation and to check the level of significance difference between SAVI, NDBI, and LST in 1987 and 2023.

RESULTS AND DISCUSSION

Spatial distribution of SAVI, NDBI, and LST in 1987: The minimum value of SAVI recorded in 1987 was -0.126, and the maximum value was 0.477. This range of values was used to generate four land cover classes based on the observed pixel values. Careful inspection of the pixels with the inspection tool in ArcMap shows that water bodies have negative values and values close to zero; bareland and built-up areas have values of 0 – 0.19; sparse vegetation has values of 0.19 – 0.24; and dense vegetation has values greater than 0.24 (da Silva Soares *et al*., 2023).

In the result (Figure 3a), bareland and built-up areas were classified together as they both showed similar SAVI values. Figure 3b shows the NDBI range; the minimum and maximum NDBI values recorded in 1987 range from -0.186 to 0.678, respectively. Negative values of NDBI represent water bodies and vegetation cover, while positive values indicate areas without water or vegetation, in this case, bareland and built-up areas. In this result, bareland and built-up were classified together as they both show similar NDBI values (Abdalkadhum *et al*., 2021; Shah *et al*., 2022). Figure 3c shows the LST result for the year 1987; the minimum LST recorded was 27.18 ºC, while the maximum value of LST was 46.4 ºC. After performing pixel observation, the range of values observed was used to classify the map, and the results show that a large area of land experienced high temperatures ranging from 32 ºC to 46.4 ºC, with the exception of water bodies and dense vegetation, which show a temperature range of 27.18 ºC to 32 ºC.

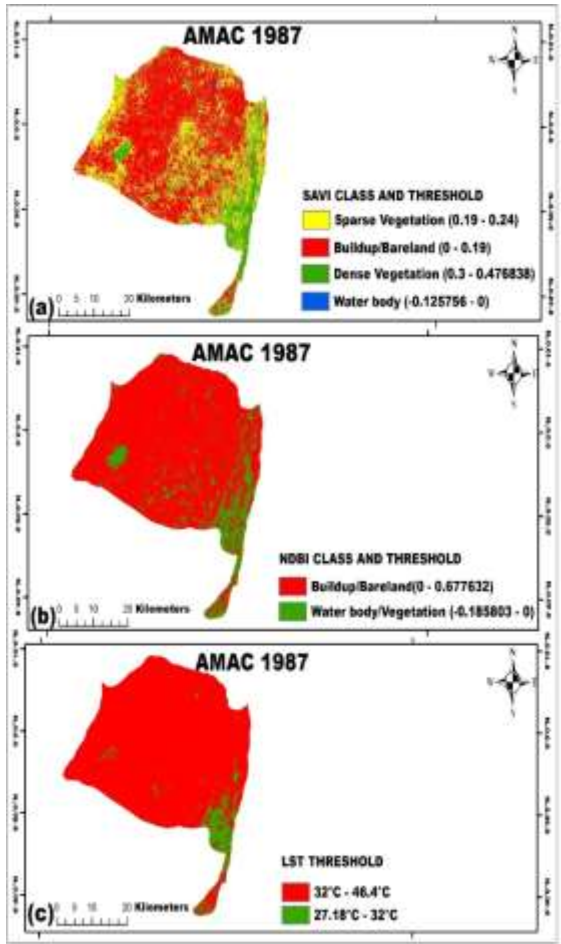

Fig 3: showing a (SAVI), b (NDBI), and c (LST) for AMAC 1987

Spatial distribution of SAVI, NDBI, and LST in 2023: The minimum and maximum values of SAVI recorded in 2023 range from -0.253 to 0.71. This range of values was used to generate four land cover classes based on the observed pixel values. Careful inspection of the pixels with the inspection tool in ArcMap shows that water bodies have negative values and values close to zero; bareland and built-up areas have values of 0 – 0.19; sparse vegetation has values of 0.20 – 0.4; and dense vegetation has values of 0.41 – 0.71 (da Silva Soares *et al*., 2023). In the result (Figure 4a), bareland and built-up areas were classified together as they both showed similar SAVI values. By observing the band composite in Figure 2b, it is clear that the built-up area increased towards the northeast region. This is true for the classified SAVI map of 2023, as the built-up/bareland class is mostly concentrated in the northeast. Hence, it is therefore right to say that sparse vegetation increased in AMAC in 2023 at the expense of bareland.

Dense vegetation also increased in the southern part of AMAC. Figure 4b shows the NDBI range; the minimum and maximum NDBI values recorded in 2023 range from -0.308 to 0.619, respectively. As earlier stated, negative values of NDBI represent water bodies and vegetation cover, while positive values indicate areas without water or vegetation, in this case bareland and built-up areas. In this result, bareland and built-up were classified together as they both show similar NDBI values. From Figure 4c, the minimum LST recorded was 23.89 ºC, while the maximum value of LST was 46.57 ºC. Consequent upon performing pixel observation, the range of values observed was used to classify the map, and the results show that there was a reduction in temperature in certain regions due to the increase in vegetation. For example, regions towards the south and southwest that experienced high temperatures in 1987 became cooler in 2023. In the same way, the main city that experienced high temperatures in 1987 started experiencing lower temperatures due to the presence of vegetation. LST can be affected by the nature of land surface cover, ranging from the bare ground to vegetation cover types (Zhang *et al*., 2009). The results show that LST values have decreased in certain areas due to an increase in vegetation.

Relationship between SAVI, NDBI, and LST in 1987 and 2023: To better understand the relationships between SAVI, NDBI, and LST, sample points (Figure 1) from built-up/bareland, sparse vegetation, dense vegetation, and water bodies were used to investigate the relationships between SAVI and LST and the relationship between NDBI and LST. Pearson correlation (Tables 1 and 2) was used to find the relationship between SAVI, NDBI, and LST. For correlation analysis, a total of 195 sampling points were extracted using the fishnet method from the raster data of SAVI, NDBI, and LST in 1987 and 2023, respectively. These sampling points were uniformly collected to represent all the groups classified by the SAVI, NDBI, and LST thresholds. From Table 1, there is a strong negative relationship (-.772) between SAVI and LST in 1987 and a moderately strong positive relationship (.645) between NDBI and LST. From Table 2, there is a weak negative relationship (-.389) between SAVI and LST in 2023 and a moderately strong positive relationship (.621) between NDBI and LST. These correlations were significant at the 0.01 level. The moderately strong positive relationship found between NDBI and LST indicates that built-up or bareland areas are generating high land surface temperature. While the negative correlation between SAVI and LST shows that vegetation cover plays a key role in lowering the land surface temperature. Elevated SAVI values signify the existence of dense vegetation, whereas elevated NDBI values signify the existence of both built-up areas and barelands.

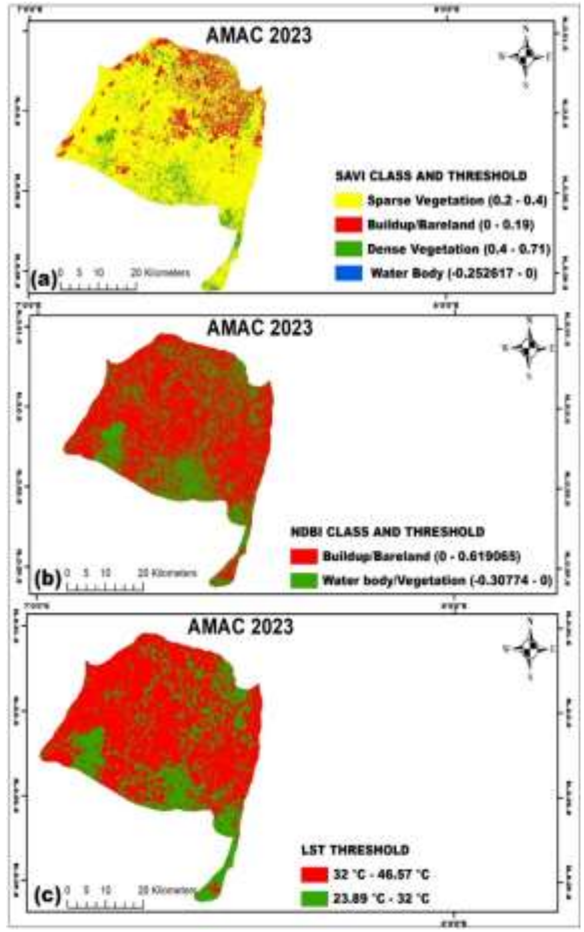

Fig 4 showing a (SAVI), b (NDBI), and c (LST) for AMAC 2023

Table 1: Correlation between SAVI, NDBI and LST in 1987

Indices		LST
SAVI	Pearson Correlation	-.772**
	Sig. (2-tailed)	.000
NDBI	Pearson Correlation	.645**
	Sig. (2-tailed)	.000

**. Correlation is significant at the 0.01 level (2-tailed).

Table 2: Correlation between SAVI, NDBI and LST in 2023

Indices		LST
SAVI	Pearson Correlation	-.389**
	Sig. (2-tailed)	.000
NDBI	Pearson Correlation	.621**
	Sig. (2-tailed)	.000

**. Correlation is significant at the 0.01 level (2-tailed).

Levels of significant difference in SAVI, NDBI, and LST between 1987 and 2023: From Tables 3, 4, and 5, there was a significant difference ($P<0.01$) between the SAVI values extracted from the same points in 1987 and the SAVI values of 2023. In the same way, there was a significant difference ($P<0.01$) found between the NDBI of 1987 and the NDBI of 2023. In addition, there was a significant difference ($P<0.01$) found between the LST values of 1987 and the LST values of 2023 extracted from the same points.

Table 3: Paired Samples Statistics for SAVI

	Mean	N	Std. Deviation	Std. Error Mean	Sig. (2 tailed)
SAVI 1987	0.17903	195	0.048414	0.003467	P value < 0.01
SAVI 2023	0.29754	195	0.09434	0.006756	.(000)

P<0.01 = highly significant

Table 4: Paired Samples Statistics for NDBI

	Mean	N	Std. Deviation	Std. Error Mean	Sig. (2 tailed)
NDBI 1987	0.05028	195	0.042654	0.003055	P value < 0.01
NDBI 2023	0.01461	195	0.056092	0.004017	(.000)

P<0.01 = highly significant

Table 5: Paired Samples Statistics for LST

	Mean	N	Std. Deviation	Std. Error Mean	Sig. (2 tailed)
LST 1987	36.5546	195	2.57746	0.18458	P value < 0.01
LST 2023	32.6634	195	1.60834	0.11518	(.000)

P<0.01 = highly significant

As reported by Sarkar and Patra (2022), built-up areas and bareland have high NDBI values. One will expect the NDBI value to rise due to land conversion to developed land with industrial and commercial buildings, residential buildings, and roads; however, this was not the case in AMAC, as vegetation cover rose alongside built-up land at the expense of bare land, reducing the mean value of NDBI (Table 4).

NDBI can identify the density of urban and built-up areas (Yasin *et al*., 2020). According to Asyraf *et al*. (2020), a higher NDBI density indicates densely populated metropolitan regions with impermeable surfaces. High NDBI values (more built areas and bareland) have a high LST value, and vice versa (Raynolds *et al*., 2008). This also implies that areas with low LST values have correspondingly high SAVI values. The high levels of LST in built-up and bareland might have been so because built-up areas are characterized by a high concentration of buildings, roads, pavements, and high-rise structures that contribute to higher LST (Voogt, 2004). Alteration of vegetation cover is one of the likely factors responsible for the rise in LST (Kumar and Shekhar, 2015).

In a study conducted by Babalola and Akinsanola (2016), bare surfaces exhibited relatively higher LST values than other land cover classes, probably because they tend to have a sparse or complete absence of vegetation. Increasing urban vegetation cover is an often suggested mitigation approach to lower city temperatures (De Abreu-Harbich *et al*., 2015; Wang *et al*., 2016; Morakinyo *et al*., 2017). Increased vegetation cover has the effect of lowering the temperature of the surroundings in its shadow, thus reducing LST (Meili *et al*., 2021). Chow *et al*. (2016) and Middel *et al.* (2016) opined that the presence of vegetation in cities could decrease air temperature through shade provision, which is beneficial to hot cities.

Conclusion: Unlike other researches, which often reports high losses of vegetation and increases in land surface temperature in cities, this research reveals an increase in vegetation cover and a decrease in land surface temperature in Abuja Municipal Area Council between 1987 and 2023. For continuous urban sustainability, relevant agencies and urban planners should look towards planting trees in the northeast, east, and northwest regions as one of the best ways to reduce urban temperature.

REFERENCES

Abdalkadhum, AJ; Salih, MM; Jasim, OZ (2021). The correlation among land cover spectral indices and surface temperature using remote sensing techniques. In IOP Conference Series: *Mater. Sci. Eng. A.* 1090 (1): 012024. DOI: 10.1088/1757-899X/1090/1/012024

Adewale, FO; Martins, M (2019). Assessment of the Relationship between Urban Growth and surface Temperature in Abuja Municipal Area Council. *FUDMA J. Sci.* 3 (3): 309 – 327.

Adeyeri, OE; Okogbue, EC; Ige, SO; Ishola, KA (2015). Estimating the Land Surface Temperature over Abuja using different Landsat sensors. Proceedings of the Climate Change. *Environ. Chall Sustain. Dev.* 305 - 310.

Ahmadi, H; Nusrath, A (2012). Vegetation change Detection of Neka River in Iran by using remote sensing and GIS. *J Geogr. Geol.* 2 (1): 58 - 67.

Amaechi, CF; Enuneku, AA; Okhai, SO; Okoduwa, KA (2023). Geospatial Assessment of Deforestation in the Federal Capital Territory Abuja, Nigeria from 1987 to 2021. *J. Appl. Sci. Environ. Manage.* 27(11): 1881-1888.

Anandababu, D; Purushothaman, BM; Suresh, BS (2018). Estimation of land surface temperature using Landsat 8 data. *Int. J. Adv. Sci. Res.* 4 (2): 177 - 186. DOI: 10.4314/jasem.v27i11.13

Andhale, AN; Parmar, HV; Pappu KP (2020). Soil adjusted vegetation index (SAVI), in the Uben river basin of Gujarat. *Int. J. Chem. Stud.* 8 (5): 693 - 698. DOI: 10.22271/chemi.2020.v8.i5j.10381

Arifin, SS; Hamzah, B; Mulyadi, R; Rasyid, AR (2022). Effects of Vegetation on Urban Heat Island Using Landsat 8 OLI/TIRS Imagery in Tropical Urban Climate. *Civ. Eng. Archit.* 10: 395 - 405. DOI: 10.13189/cea.2022.100134

Asyraf, MS; Damayanti, A; Dimyati, M (2020). The effect of building density on land surface temperature, (Case Study: Turikale District, Maros Regency). In IOP Conference Series: *Environ. Earth Sci*. 500 (1): 012061. DOI: 10.1088/1755-1315/500/1/012061

Avdan, U; Jovanovska, G (2016). Algorithm for automated mapping of land surface temperature using LANDSAT 8 satellite data. *J. Sens.* 2016: 1 - 8. DOI: https://doi.org/10.1155/2016/1480307

Babalola, OS; Akinsanola, AA (2016). Change Detection in Land Surface Temperature and Land Use Land Cover over Lagos Metropolis, Nigeria. *Remote Sens. GIS*. 5 (3): 6 - 10. DOI: 10.4172/2469-4134.1000171

Balogun, O (2001). The Federal Capital Territory of Nigeria: a geography of its development. Ibadan university press.

Chow, WT; Akbar, SNABA; Heng, SL; Roth, M (2016). Assessment of measured and perceived microclimates within a tropical urban forest. *Urban For. Urban Green.* 16: 62 - 75. DOI: https://doi.org/10.1016/j.ufug.2016.01.010

da Silva Soares, LC; Souza, PGC; Rodrigues, SDA; Perpétuo, RCS; Perpétuo, IA (2023). Modeling of the land surface temperature as a function of the soil-adjusted vegetation index. *Revista Agrogeoambiental*. e20231723 - e20231723. DOI: 10.18406/2316-1817v15nunico20231723

Dar, I; Qadir, J; Shukla, A (2019). Estimation of LST from multi-sensor thermal remote sensing data and evaluating the influence of sensor characteristics. *Ann. GIS.* 25 (3): 263 - 281. DOI: https://doi.org/10.1080/19475683.2019.1623318

De Abreu-Harbich, LV; Labaki, LC; Matzarakis, A (2015). Effect of tree planting design and tree species on human thermal comfort in the tropics. *Landsc. Urban Plan*. 138: 99 - 109. DOI: 10.1016/j.landurbplan.2015.02.008

Fabolude, G; Aighewi, IT (2022). Evaluation of the Extent of Land Use-Land Cover Changes of Benin City, Edo State, Nigeria from 1987-2019. *J. Appl. Sci. Environ. Manage.* 26 (8): 1443 - 1450. DOI: 10.4314/jasem.v26i8.18

Fu, P; Weng, Q (2016). A time series analysis of urbanization induced land use and land cover change and its impact on land surface temperature with Landsat imagery. *Remote Sens. Environ.* 175: 205 - 214. DOI: https://doi.org/10.1016/j.rse.2015.12.040

Guha, S; Govil H; Dey A; Gill N (2020). A case study on the relationship between land surface temperature and land surface indices in Raipur City, India. *Geografisk Tidsskrift-Danish J. Geogr.* 120 (1): 35 – 50. DOI: https://doi.org/10.1080/00167223.2020.1752272

Guha, S; Govil, H; Dey, A; Gill, N (2018). Analytical study of land surface temperature with NDVI and NDBI using Landsat 8 OLI and TIRS data in Florence and Naples city, Italy. *Eur. J. Remote Sens.* 51 (1): 667 - 678. DOI: https://doi.org/10.1080/22797254.2018.1474494

Hari, KK (2018). Study of Normalized Difference Built-Up (NDBI) Index in Automatically Mapping Urban Areas from Landsat TM Imagery. *Int. J. Sci. Res.* 7 (1): 1 - 9.

Huang, S; Tang, L; Hupy, JP; Wang, Y; Shao, G (2021). A commentary review on the use of normalized difference vegetation index (NDVI) in the era of popular remote sensing. *J. For. Res.* 32 (1): 1 - 6. DOI: https://doi.org/10.1007/s11676-020-01155-1

Huete, ARA (1988). Soil-Adjusted Vegetation Index (SAVI). *Remote Sens. Environ.* 25 (3): 205 - 309. DOI: https://doi.org/10.1016/0034-4257(88)90106-X

Ifatimehin, OO; Ujoh, F; Magaji, JY (2009). An evaluation of the effect of land use/cover change on the surface temperature of Lokoja town, Nigeria. *Afr. J. Environ. Sci. Technol*. 3 (3): 086 - 090.

Karaburun, AA; Bhandari, K (2010). Estimation of C factor for soil erosion modelling using NDVI in Buyukcekmece watershed, Ozean. *J applied sciences.* 3: 77 - 85.

Kolokotroni, M; Giannitsaris, I; Watkins, R (2006). The effect of the London urban heat island on building summer cooling demand and night ventilation strategies. *Sol. Energy* 80 (4): 383 – 392. DOI: https://doi.org/10.1016/j.solener.2005.03.010

Kumar, D; Shekhar, S (2015). Statistical analysis of land surface temperature–vegetation indexes relationship through thermal remote sensing. *Ecotoxicol. Environ. Saf.* 121: 39 - 44. DOI: https://doi.org/10.1016/j.ecoenv.2015.07.004

Landsat 7 Science Data Users Handbook, (2010). National Aeronautics and Space Administration. 117–120. Landsat Project Science Office at NASA's Goddard Space Flight Center: Greenbelt, MD, USA, 2010.

Le Joseph, G (2020). Investigating Ndvi Based Vegetation Dynamics and Its Relation to Environmental Variables in Parambikulam Forest, Kerala (Doctoral dissertation, Kerala Forest Research Institute).

Li, J; Pei, Y; Zhao, S; Xiao, R; Sang, X; Zhang, C (2020). A review of remote sensing for environmental monitoring in China. *Remote Sens.* 12 (7): 1130. DOI: https://doi.org/10.3390/rs12071130

Mabogunje, AL (1976). Cities and African Development (Studies of African Resources). Available online at https://search.worldcat.org/title/cities-and-african-development/oclc/13835394. Retrieve January 18, 2024.

Malik, MS; Shukla, JP; Mishra, S (2019). Relationship of LST, NDBI and NDVI using landsat-8 data in Kandaihimmat watershed, Hoshangabad, India. *Indian J. Geo-Mar. Si.* 48 (01): 25 - 31.

Meili, N; Acero, JA; Peleg, N; Manoli, G; Burlando, P; Fatichi, S (2021). Vegetation cover and plant-trait effects on outdoor thermal comfort in a tropical city. *Build. Environ*. 195: 107733. DOI: https://doi.org/10.1016/j.buildenv.2021.107733

Middel, A; Selover, N; Hagen, B; Chhetri, N (2016). Impact of shade on outdoor thermal comfort—a seasonal field study in Tempe, Arizona. *Int. J. Biometeorol*. 60: 1849 - 1861. DOI: 10.1007/s00484-016-1172-5

Mohan, M; Kandya, A (2015). Impact of urbanization and land-use/land-cover change on diurnal temperature range: A case study of tropical urban airshed of India using remote sensing data. *Sci. Total Environ.* 506: 453 - 465. DOI: https://doi.org/10.1016/j.scitotenv.2014.11.006

Morakinyo, TE; Kong, L; Lau, KKL; Yuan, C; Ng, E (2017). A study on the impact of shadow-cast and tree species on in-canyon and neighborhood's thermal comfort. *Build. Environ*. 115: 1 - 17. DOI: https://doi.org/10.1016/j.buildenv.2017.01.005

National Bureau of Statistics (NBS) (2017) Annual Abstract. Available online at https://nigerianstat.gov.ng/pdfuploads/Annual%20Abstract%20of%20Statistics,%202017 .pdf. Retrieve January 18, 2024.

NPC (2006). Population and Housing Census Enumerators Manual. Federal Republic of Nigeria, National Population Commission, Nigeria.

Qiu, GY; Li, HY; Zhang, QT; Wan, CHEN; Liang, XJ; Li, XZ (2013). Effects of evapotranspiration on mitigation of urban temperature by vegetation and urban agriculture. *J. Integr. Agric.* 12 (8): 1307 - 1315. DOI: https://doi.org/10.1016/S2095-3119(13)60543-2

Faqe Ibrahim, GR; (2017). Urban land use land cover changes and their effect on land surface temperature: Case study using Dohuk City in the Kurdistan Region of Iraq. *Climate*. 5 (1): 13. DOI: **https://doi.org/10.3390/cli5010013**

Raynolds, MK; Comiso, JC; Walker, DA; Verbyla, D (2008). Relationship between satellite-.derived .Land Surface Temperatures, arctic vegetation types, and NDVI. *Remote Sens. Environ*. 112 (23): 1884 – 1894.

Rhyma, PP; Norizah, K; Hamdan, O; Faridah-Hanum, I; Zulfa, AW (2020). Integration of normalised different vegetation index and Soil-Adjusted Vegetation Index for mangrove vegetation delineation. *Remote Sens. Appl. Soc. Environ.* 17: 100280. DOI: https://doi.org/10.1016/j.rsase.2019.100280

Ru, C; Duan, SB; Jiang, XG; Li, ZL; Jiang, Y; Ren, H; Gao, M (2021). Land surface temperature retrieval from Landsat 8 thermal infrared data over urban areas considering geometry effect: Method and application. *IEEE Trans Geosci Remote Sens*. 60: 1-16. DOI: 10.1109/TGRS.2021.3088482

Saleem, MS; Ahmad, SR; Javed, MA (2020). Impact assessment of urban development patterns on land surface temperature by using remote sensing techniques: a case study of Lahore, Faisalabad and Multan district. *Environ. Sci. Pollut. Res.* 27 (32): 39865 - 39878.

Sarkar, B; Patra, S (2022). A Geospatial Analysis of the Relationship between Land Surface Temperature and Land Use/Land Cover Indices in Raiganj Municipality, West Bengal, India. DOI: https://doi.org/10.21203/rs.3.rs-1497635/v1.

Shah, SA; Kiran, M; Nazir, A; Ashrafani, SH (2022). Exploring NDVI and NDBI relationship using Landsat 8 OLI/TIRS in Khangarh taluka, Ghotki. *Malays. J. Anim. Sci.* 6 (1): 08 - 11.

Touristlink (2013). Abuja Nigeria Tourist Information'. Available online at Touristlink.com. Retrieve January 18, 2024.

Twumasi, YA; Merem, EC; Namwamba, JB; Mwakimi, OS; Ayala-Silva, T; Frimpong, DB; Mosby, HJ (2021). Estimation of land surface temperature from Landsat-8 OLI thermal infrared satellite data. A comparative analysis of two cities in Ghana. *Advances Remote Sens.* 10 (4): 131 - 149. DOI: 10.4236/ars.2021.104009

Usman, LS; Lay, U (2013). The Dynamic of land Cover Change in Abuja City, Federal Capital Territory, Nigeria. *Confluence J. Environ. Stud*. 8 (1597-5827): 14 - 24.

Vani, V; Mandla, VR (2017). Comparative study of NDVI and SAVI vegetation indices in Anantapur district semi-arid areas. *Int. J. Civ. Eng. Technol*. 8 (4): 559 - 566. DOI: http://iaeme.com/Home/issue/IJCIET?Volume=8&Issue=4

Voogt, JA (2004). Urban Heat Island: hotter cities. *Remote Sens. Environ.* 86 (3): 370 – 384. DOI: http://www.actionbioscience.org/environment/voogt.html

Wang, F; Qin, Z; Song, C; Tu, L; Karnieli, A; Zhao, S (2015). An improved mono-window algorithm for land surface temperature retrieval from Landsat 8 thermal infrared sensor data. *Remote sen*. 7 (4): 4268 - 4289. DOI: **https://doi.org/10.3390/rs70404268**

Wang, ZH; Zhao, X; Yang, J; Song, J (2016). Cooling and energy saving potentials of shade trees and urban lawns in a desert city. *Appl. Energy*. 161: 437 - 444. DOI: https://doi.org/10.1016/j.apenergy.2015.10.047

Xian, G; Crane, M (2006). Evaluation of Urbanization Influence on Urban Climate with Remote Sensing and Climate Observations. National Centre for Earth Resources Observation and Science, Sioux Falls, SD. 57198. 1 – 7

Yasin, MY; Abdullah, J; Noor, NM; Yusoff, MM; Noor, NM (2022). Landsat observation of urban growth and land use change using NDVI and NDBI analysis. In IOP Conference Series: *Environ. Earth Sci*. 1067 (1): 012037. DOI: 10.1088/1755-1315/1067/1/012037

Zareie S; Khosravi H; Nasiri A (2016). Derivation of land surface temperature from landsat thematic mapper (TM) sensor data and analysing relation between land use changes and surface temperature. *Solid Earth Discuss.* 1 – 15. DOI: doi:10.5194/se-2016-22

Zha, Y; Gao, J; Ni, S (2003). Use of normalized difference built-up index in automatically mapping urban areas from TM imagery. *Int. J. Remote Sens.* 24 (3): 583 − 594. DOI: https://doi.org/10.1080/01431160304987

Zhang, Y; Odeh, IO; Han, C (2009). Bi-temporal characterization of land surface temperature in relation to impervious surface area, NDVI and NDBI, using a sub-pixel image analysis. *Int. J. Appl. Earth Obs. Geoinf.* 11 (4): 256 - 264. DOI: https://doi.org/10.1016/j.jag.2009.03.001